Role of zinc content and the catalytic efficiency of B1 metallo β-lactamases

Matteo Dal Peraro,[†]* Alejandro J. Vila,[§] Paolo Carloni[‡] and Michael L. Klein[†]

[†]Center for Molecular Modeling, University of Pennsylvania, 231 S. 34th Street, Philadelphia, PA 19104, USA

[‡]International School for Advanced Studies, SISSA-ISAS, via Beirut 4, Trieste, Italy

[§]Molecular Biology Division, IBR, CONICET, and Biophysics Section, Universidad Nacional de Rosario, Suipacha 531, S2002LRK Rosario, Argentina

SUPPLEMENTARY INFORMATION

*To whom correspondence should be addressed:

matteodp@cmm.upenn.edu, phone: 1-215-898-9347, fax: 1-215-573-6233

MD structural analysis of CcrA adducts and comparison with BcII adducts[50]

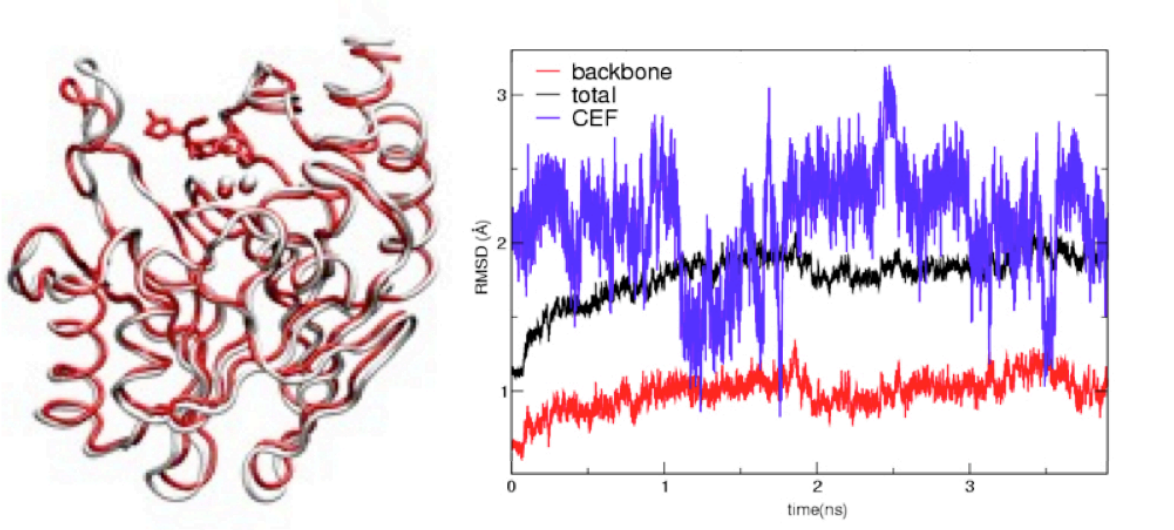

Figure 1SI. CcrA-CEF RMSD. Left. Superposition of the X-ray 1znb structure (in gray) and the MD average structure of CcrA-CEF (in red). **Right.** RMSD of CcrA relative to initial X-ray structure is plotted *vs.* time. The RMSD of CEF substrate is also reported in blue.

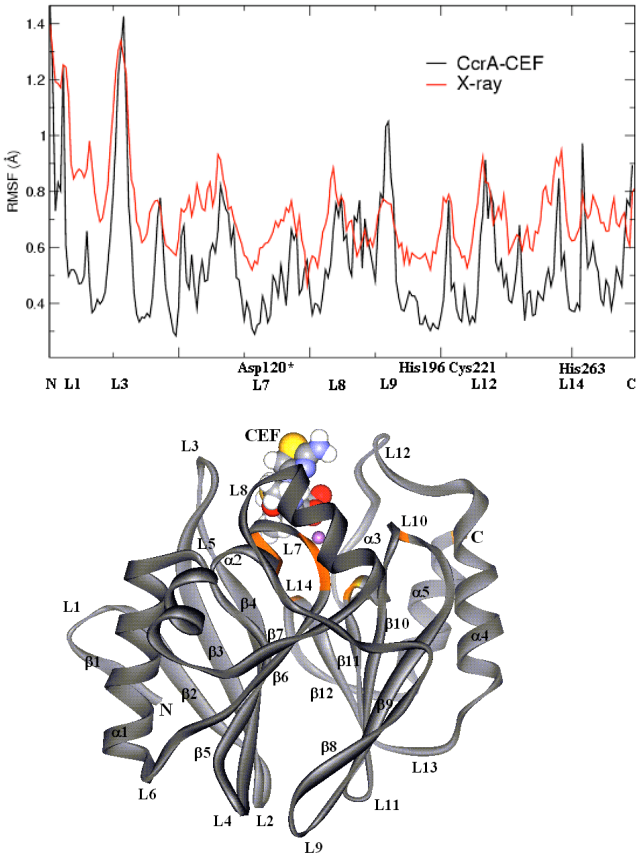

Figure 2SI. CcrA-CEF RMSFs. The calculated and experimentally derived RMS fluctuations per residue are compared for CcrA X-ray and MD structure. Relevant residues and loops are indicated in abscissa (Asp120* stands for His116, His118, Asp120 and Arg121 residues motif, labels are reported in the CcrA cartoon at the bottom).

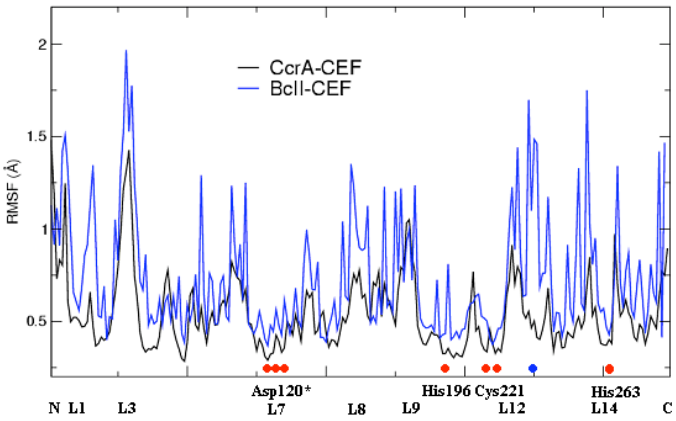

Figure 3SI. RMSFs CcrA-CEF vs. BcII-CEF. The calculated RMS fluctuations per residue of CcrA-CEF model are compared with those of the monozinc MD BcII-CEF structure (50). Relevant residues and loops are indicated in abscissa (Asp120* stands for His116, His118, Asp120 and Arg121 residues). Red dots indicated zinc ligands, whereas blue dot L12, and Asn233 residue in particular.

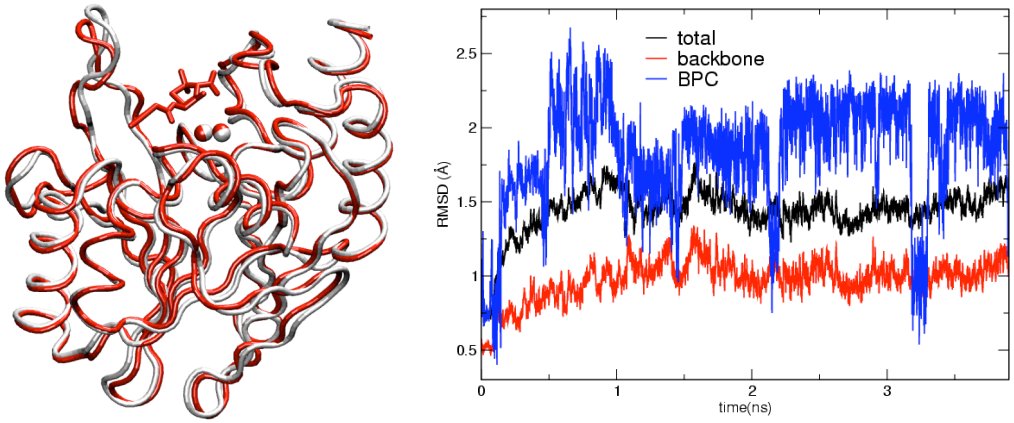

Figure 4SI. CcrA-BPC RMSD. Left. Superposition of the X-ray structure (in gray) and the MD average structure of CcrA-BPC (in red). **Right.** RMSD of CcrA relative to initial X-ray structure is plotted *vs.* time. The RMSD of BPC substrate is also reported in blue relative to its docked initial position.

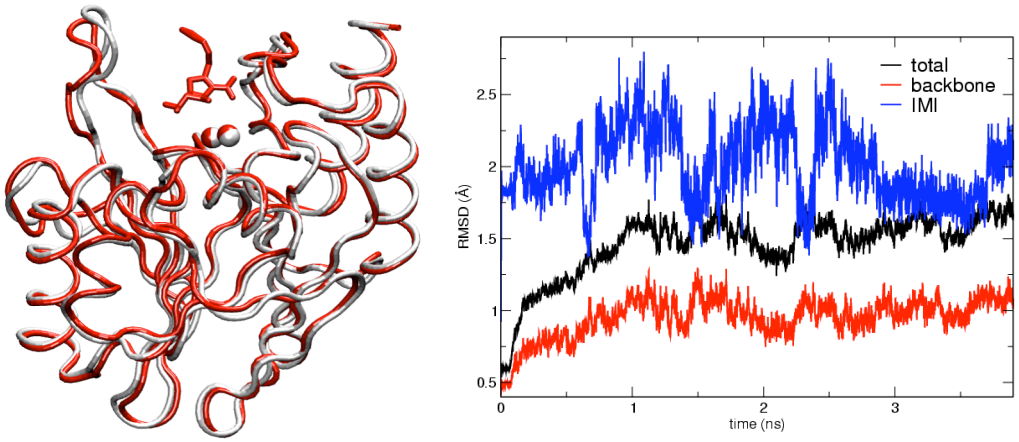

Figure 5SI. CcrA-IMI RMSD. Left. Superposition of the X-ray structure (in gray) and the MD average structure of CcrA-IMI (in red). **Right.** RMSD of CcrA relative to initial X-ray structure is plotted *vs.* time. The RMSD of IMI substrate is also reported in blue relative to its docked initial position.

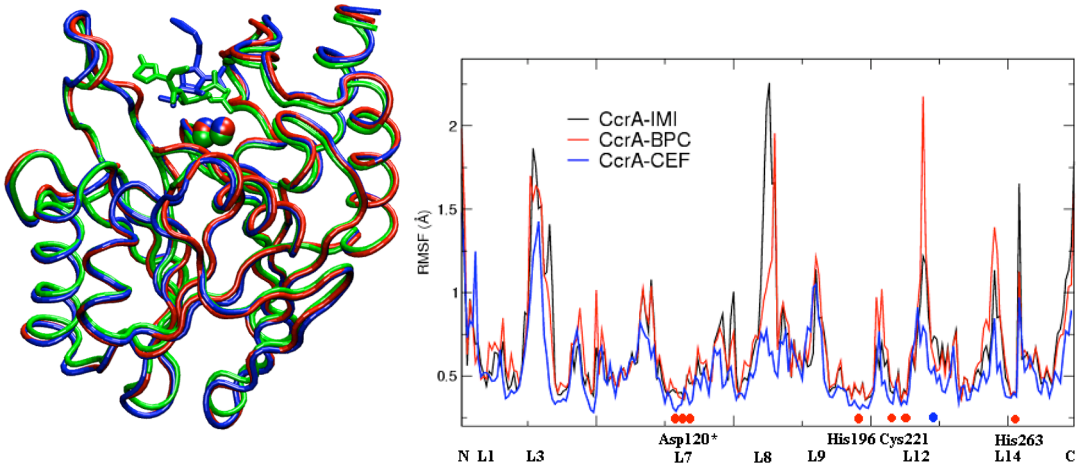

Figure 6SI. Left. Superposition of the MD-average structures (CcrA-CEF in green, CcrA-BPC in red, CcrA-IMI in blue). **Right.** RMSF's of CcrA MD adducts. Relevant residues and loops are indicated in abscissa (Asp120* stands for His116, His118, Asp120 and Arg121 residues, ref. 50).

CcrA-CEF adduct

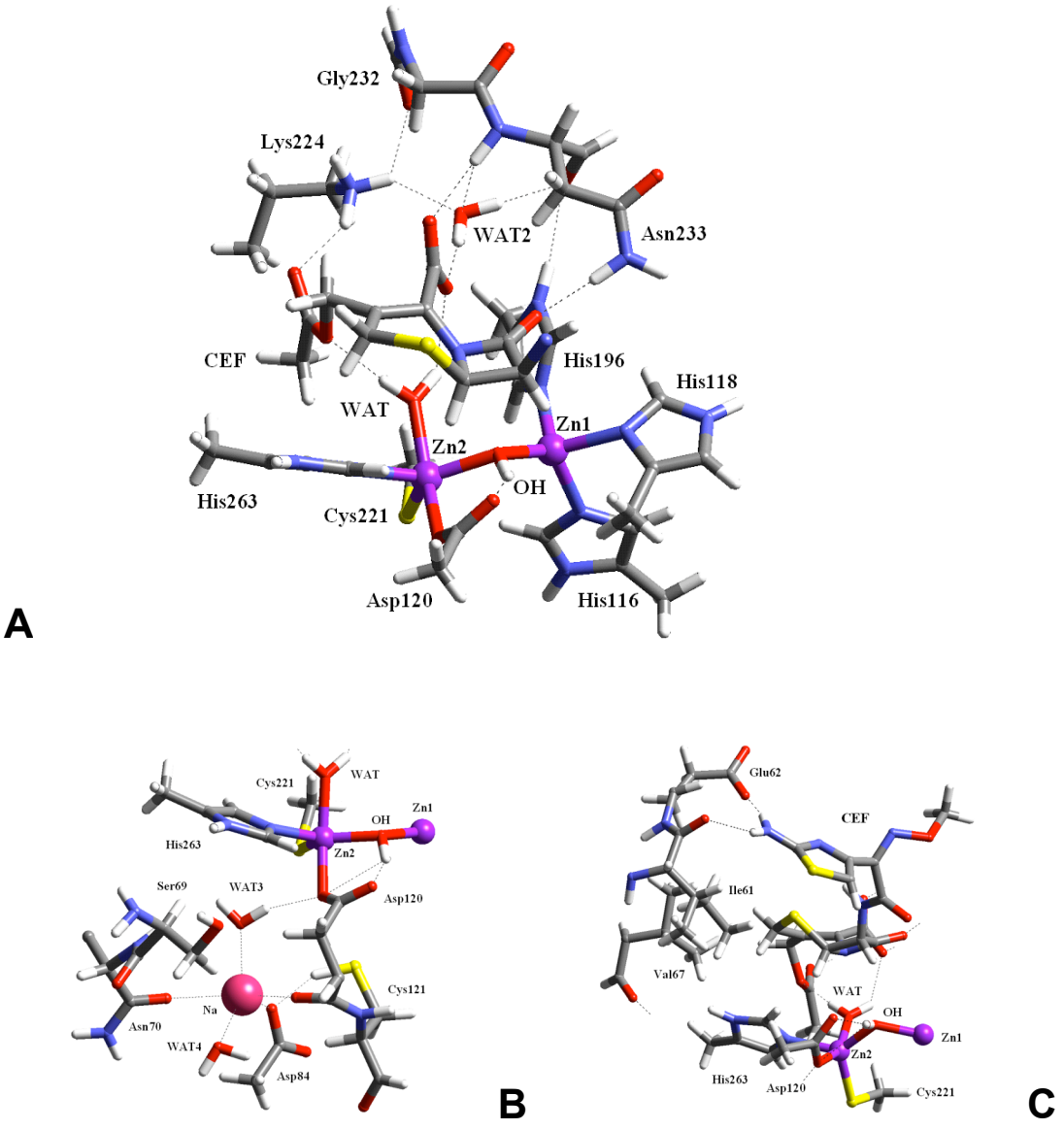

Figure 7SI. A-C CcrA-CEF active site H-bonds network. A. CEF binding mode. **B.** Na+ ion solvation shell near Asp120 residue. Atoms are represented in ball-and-sticks, zinc and sodium ions as purple, and pink spheres. H-bond interactions are indicated in dashed lines.**C.** CEF interactions on loop L3.

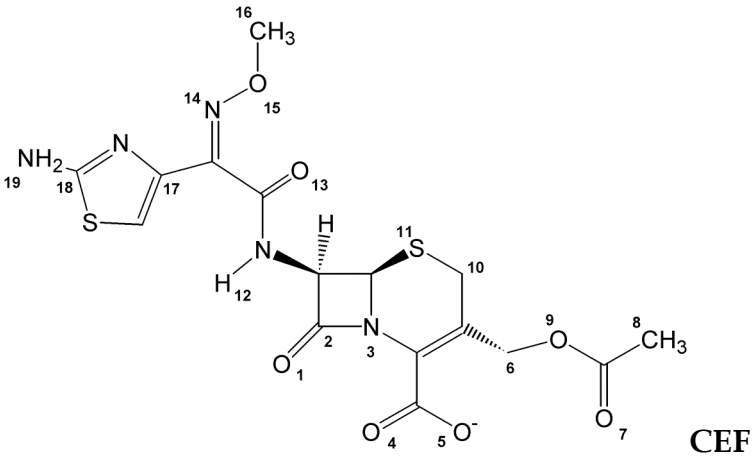

Scheme 1SI. Chemical structures of cefotaxime (CEF) (labels as used in the following tables).

H-bonds	X···H–Y	%
Oδ1@Asp120 ··· H–O@OH	2.63(9)	100
Oδ1@Asp120 ··· H–N@Asp120	2.86(9)	55
Oδ2@Asp120 ··· H–O@WAT3	2.89(16)	97
O@His118 ··· H–N@Cys121	2.93(12)	100
O@His118 ··· H–N@Ile122	3.02(15)	99
Oδ1@Asn79 ··· H–Nδ1@His116	2.82(11)	100
Oδ1@Asp236 ··· H–Nε2@His118	2.89(14)	91
Oδ2@Asp236 ··· H–Nε2@His118	3.14(19)	61
O@Asn233··· H–Nδ1@His196	3.04(19)	87
Oδ1@Asn233··· H–Oγ@Ser235	2.77(16)	61
Oδ1@Asn233··· H–N@Ser235	3.13(17)	89
O@Pro34 ··· H–Nδ2@His263	2.79(11)	100
Oδ2@Asp50… H-S@Cys221	3.24(13)	65
O1@CEF ··· H–Nδ2@Asn233	2.98(16)	90
O4@CEF ··· H–N@Asn233	3.22(20)	15
O4@CEF ··· H-WAT	2.96(21)	80
O4@CEF ··· H-WAT2	2.72(12)	87
O5@CEF ··· H–N@Asn233	2.97(16)	96
O5@CEF ··· H-WAT2	3.28(16)	25
O7@CEF ··· H–Nζ@Lys224	2.83(13)	93
O8@CEF ···H-WAT	2.93(17)	91
WAT2 ··· H–Nζ@Lys224	2.91(15)	90
O@Asn233 ··· H-WAT2	3.02(22)	66
Oδ2@Asp234 ··· H–O@wat	2.68(12)	100
Oδ1@Asp234 ··· H–O@wat	2.69(13)	95
Oδ2@Asp84 ··· H–S@Cys121	3.24(13)	65
O@Ile61 … H-N19@CEF	2.98(18)	61
Oε1@Glu62 … H-N19@CEF	2.97(20)	34
Oε2@Glu62 … H-N19@CEF	2.96(19)	52

Table 1SI. Selected active site H-bond interactions. Distances are in Å, see Figure 7SI

CEF distances	X@CEF···CcrA
O1 ··· Zn1	4.13(36)
C2 ··· O@OH	3.41(25)
N3 ··· Zn2	3.80(18)
Na ··· O@Asn70	2.42(11)
Na ··· O@Asp120	2.43(13)
Na ··· Oδ2@Asp84	2.35(10)
Na ··· H@Cys121	3.71(49)
Na ··· WAT3	2.47(15)
Na ··· WAT4	2.37(9)
S ··· Cγ2@Val67	6.06(98)
S ··· Cδ@Ile61	4.18(45)

Table 2SI. CEF principal contacts. Distances are in Å, see Figure 7SI

CcrA-BPC adduct

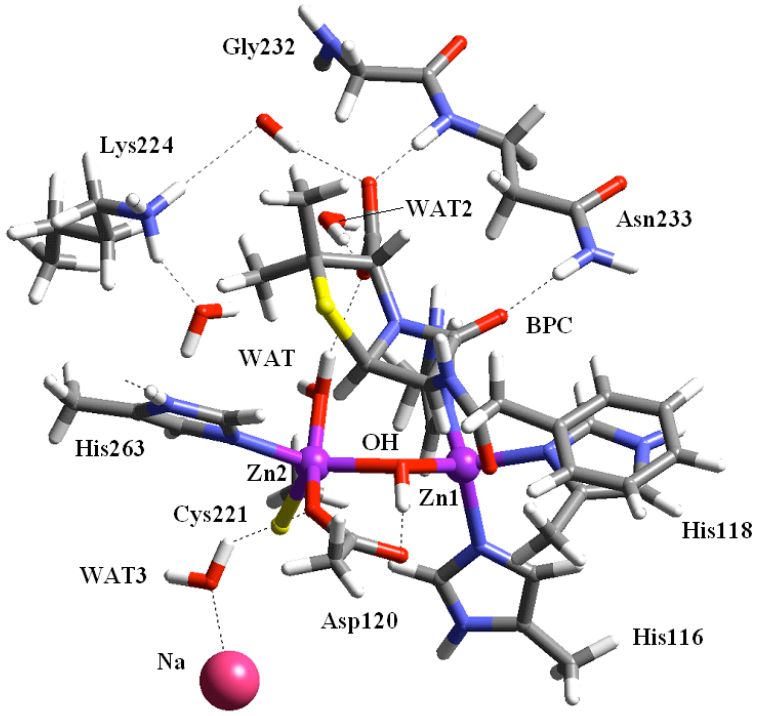

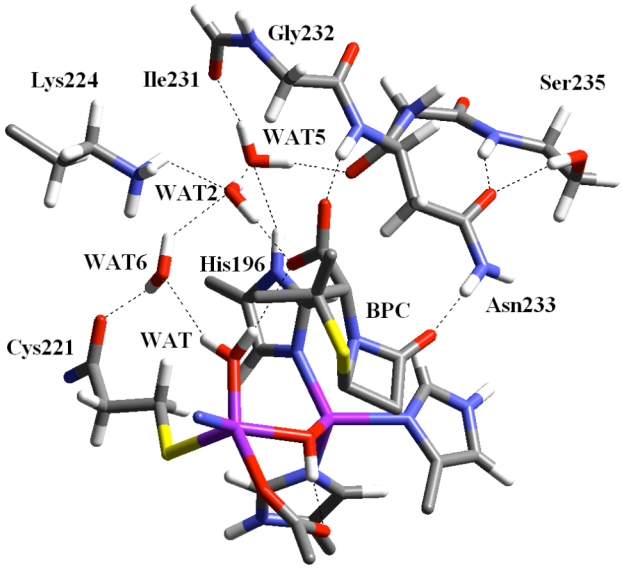

Figure 8SI. CcrA-BPC active site H-bonds network. BPC binding mode, atoms are represented in ball-and-sticks, zinc and sodium ions as purple, and pink spheres. H-bond interactions are indicated in dashed lines.

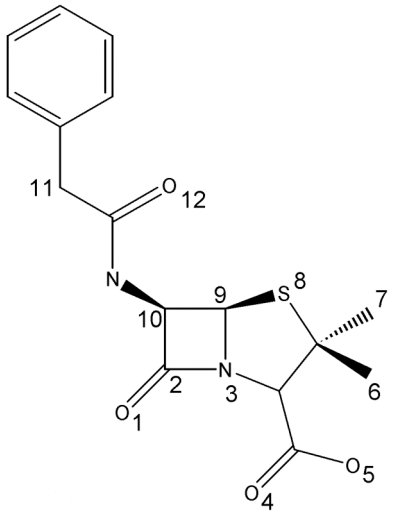

Scheme 2SI. Chemical structures of benzylpenicillin (BPC) (labels as used in the following tables).

BPC distances	X@BPC···CcrA
O1 ··· Zn1	4.50(40)
C2 ··· O@OH	3.47(20)
N3 ··· Zn2	4.24(18)
Zn2-WAT	2.00(10)
Na ... O@Asn36	2.44(13)
Na ... O@Asp120	2.49(19)
Na... Od2@Asp50	2.34(10)
Na ... WAT3	2.48(16)
Na … WAT4	2.38(10)
O4 … Nζ@Lys224	5.28(34)
C6 … Cγ2@Val67	4.95(47)
C7 … Cγ1@Val67	4.26(34)
C6 … Cγ2@Val67	4.54(39)
Ring… Cδ1@Leu61	5.24(76) min 4.3(5)
Ring… Cγ2@Leu87	5.45(71)

Table 3SI. Selected active site H-bond interactions. Distances are in Å, see Figure 8SI

CcrA-BPC H-bonds	X···H–Y	%
Oδ1@Asp120 ··· H–O@OH	2.62(10)	100
Oδ1@Asp120 ··· H–N@Asp120	2.11(18)	57
Oδ2@Asp120 ··· H–O@WAT3	2.90(18)	90
O1@CEF ··· H–Nδ2@Asn233	2.78(15)	85
O5@CEF ··· H–N@Asn233	2.87(15)	97
O4@CEF ··· H–N@Asn233	3.32(20)	19
O4@CEF ··· H–O@WAT	2.73(16)	99
O4@CEF ··· H–O@WAT2*(4)	2.71(13)	96
O@WAT2* ··· H–Nζ@Lys224	2.81(15)	83
O@Asn233 ··· H–O@WAT5	2.76(30)	91
O@WAT5··· H–Nδ@His196	2.95(21)	95

Table 4SI. BPC principal contacts. Distances are in Å, see also Figure 8SI

CcrA-IMI adduct

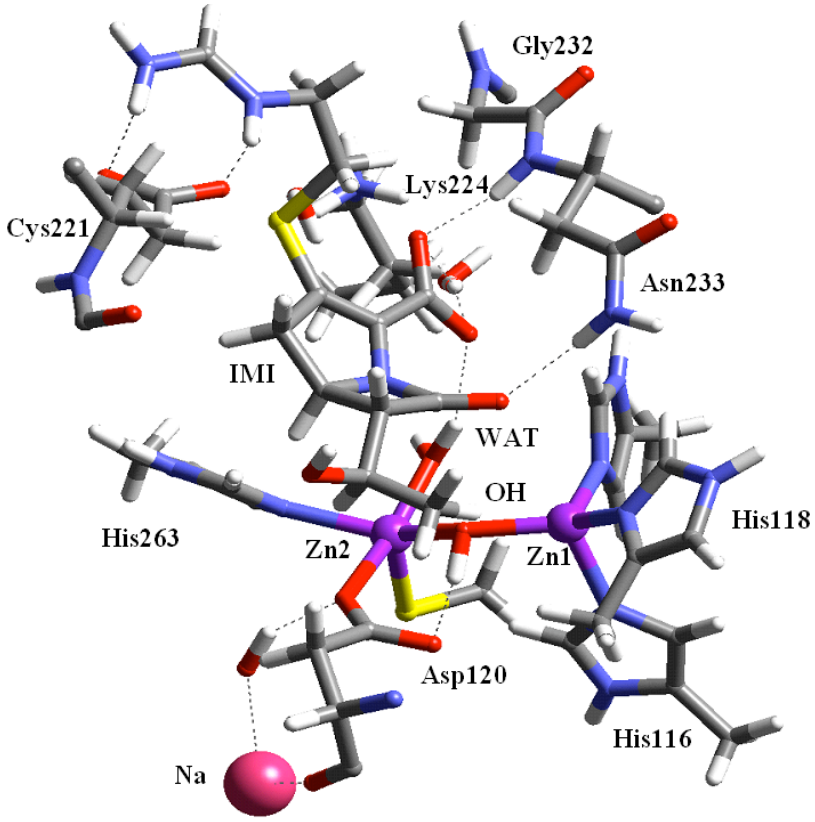

Figure 9SI. CcrA-IMI active site H-bonds network. IMI binding mode, atoms are represented in ball-and-sticks, zinc and sodium ions as purple, and pink spheres. H-bond interactions are indicated in dashed lines.

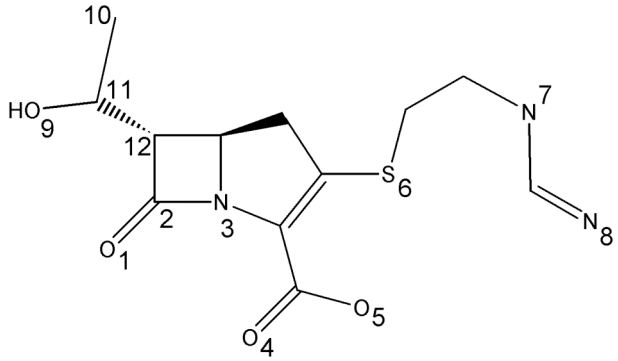

Scheme 1SI. Chemical structures of imipenem (IMI) (labels as used in the following tables).

CcrA-IMI H-bonds	X···H–Y	%
Oδ1@Asp120 ··· H–O@OH	2.63(9)	100
Oδ1@Asp120 ··· H–N@Asp120	2.91(18)	96
Oδ2@Asp120 ··· H–O@WAT3	2.93(19)	89
O1@CEF ··· H–Nδ2@Asn233	2.94(29)	80
O5@CEF ··· H–N@Asn233	2.94(22)	96
O4@CEF ··· H–O@WAT	2.77(17)	99
O4@CEF ··· H–O@WAT2	2.78(17)	97
O@WAT2 ··· H–Nz@Lys224	3.05(29)	72
O@Asn233 ··· H–O@WAT5	2.68(11)	99
O@WAT5··· H–Nd@His196	2.98(20)	94
O@WAT5···H–O@WAT2	2.78(18)	95
O@WAT2···H–O@WAT6	2.81(17)	89
O@Cys221···H–O@WAT6	2.80(22)	92
O@WAT6 … H–O@WAT	2.98(28)	66
Oe2@Glu62…H-N31	2.72(16)	86
Oe1@Glu62…H-N35	2.76(16)	87

Table 5SI. Selected active site H-bond interactions. Distances are in Å, see Figure 9SI

IMI distances	X@IMI···BcII
O1 ··· Zn1	3.68(29)
C2 ··· O@OH	3.20(17)
N3 ··· Zn2	3.88(18)
Zn2 …WAT	1.98(9)
Na ... O@Asn36	2.42(12)
Na ... O@Asp120	2.49(19)
Na... Oδ2@Asp50	2.34(10)
Na ... WAT3	2.46(17)
Na … WAT4	2.38(10)
C8 … Cγ1@Val67	4.57(46)
C8… Cδ@Leu61	6.4(6)
C8… Cδ@Leu61	6.5(6)
O4 ...N@Asn233	3.7(3)
O5 … Nζ@Lys224	4.6(5)
N8-Oε1@Glu62	2.76(16)
N7-Oε2@Glu62	2.72(16)

,

Table 6SI. IMI principal contacts. Distances are in Å, see also Figure 9SI.

Zn-ligand distances	X-ray 1znb (chain A/chain B)	MD
Zn1 ··· His116	2.14/2.22	2.17(3)
Zn1 ··· His118	2.07/2.16	2.09(3)
Zn1 ··· His196	2.08.2.01	2.07(4)
Zn1 ··· OH	1.88/1.97	1.96(2)
Zn2 ··· OH	2.06/2.13	2.06(2)
Zn2 ··· Asp120	2.25/2.15	2.21(3)
Zn2 ··· Cys221	2.30/2.35	2.31(3)
Zn2 ··· His263	2.10/2.20	2.12(4)
Zn2 ··· WAT	2.27/2.18	2.00(9)

Table 7SI. Zinc-ligand center. Comparison of zinc-ligand distances between MD (average on all the trajectories) and X-ray struture. Distances are in Å.

Solvation of the nucleophile and zinc center in CcrA and in BcII

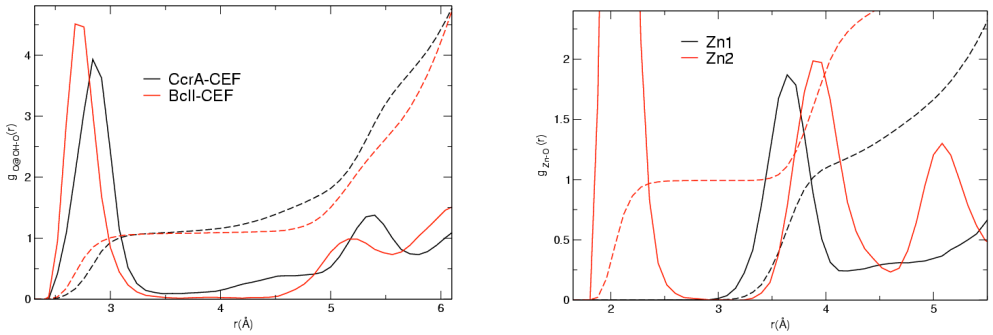

Figure 10SI. CcrA-CEF RDFs. g(r)'s of zinc ions Zn1 and Zn2 (right) and O@OH (left) with the oxygen atoms of solvent in CcrA-CEF; g(r) of OH is compared also with BcII-CEF MD model. The relative coordination numbers are reported in dashed lines and in ordinates axis.

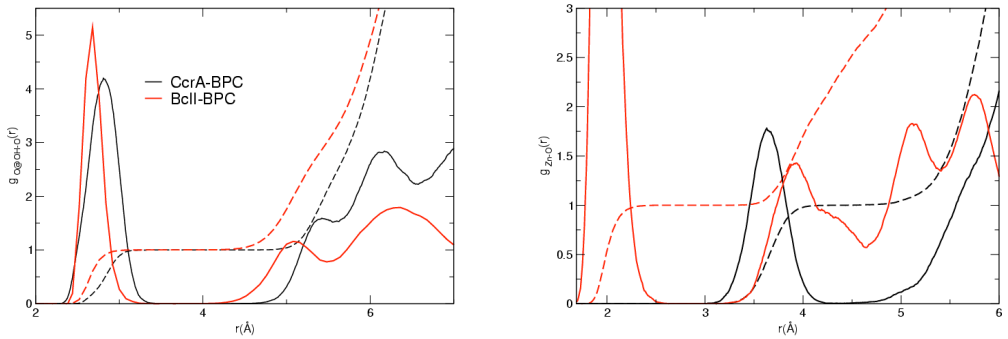

Figure 11SI. CcrA-BPC RDFs. g(r)'s of zinc ions Zn1 and Zn2 (right) and O@OH (left) with the oxygen atoms of solvent in CcrA-BPC; g(r) of OH is compared also with the BcII-BPC MD model. The relative coordination numbers are reported in dashed lines and in ordinates axis.

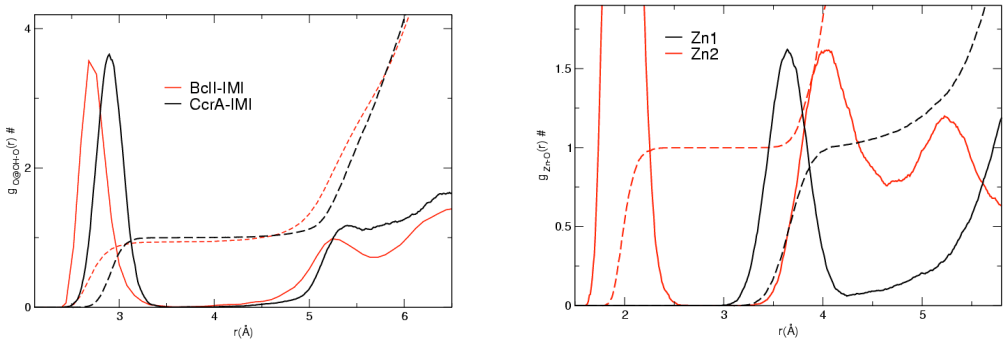

Figure 12SI. CcrA-IMI RDFs. g(r)'s of zinc ions Zn1 and Zn2 (right) and O@OH (left) with the oxygen atoms of solvent in CcrA-IMI; g(r) of OH is compared also with the same for BcII-IMI MD model. The relative coordination numbers are reported in dashed lines and in ordinates axis.